Octahedral Chromium(III) Complexes Supported by Bis(2-pyridylmethyl)amines: Ligand Influence on Coordination Geometry and Ethylene Polymerization Activity

Michael J. Carney,*,† Nicholas J. Robertson,† Jason A. Halfen,†
Lev N. Zakharov,‡ and Arnold L. Rheingold‡

Department of Chemistry, University of Wisconsin−Eau Claire, Eau Claire, Wisconsin 54702, and Department of Chemistry and Biochemistry, University of California−San Diego, La Jolla, California 92093-0358

Received July 28, 2004

This report describes the synthesis, structural characterization, and polymerization behavior of a series of chromium(III) complexes supported by bis(2-pyridylmethyl)alkylamine (BPA) ligands. The compounds are prepared in high yield by room-temperature reaction of the appropriate BPA ligand with $CrCl_3(THF)_3$. X-ray crystallographic studies reveal that the complexes' coordination geometries depend on the substituent at the 6-position of the pyridine ring. Unsubstituted ligands yield *fac*-{*N*-propyl-*N*,*N*-di(2-pyridylmethyl)amine}-$CrCl_3$ (**6A**) and *fac*-{*N*-hexyl-*N*,*N*-di(2-pyridylmethyl)amine}$CrCl_3$ (**6B**), whereas 6-methyl-substituted ligands produce *mer*-{*N*-propyl-*N*,*N*-di(6-methyl-2-pyridylmethyl)amine}$CrCl_3$ (**6C**) and *mer*-{*N*-hexyl-*N*,*N*-di(6-methyl-2-pyridylmethyl)amine}$CrCl_3$ (**6D**). Moreover, ethylene polymerization studies indicate that, upon activation by methylalumoxane, the *fac* derivatives are 30−40 times more active than their *mer* counterparts.

Introduction

Chromium catalysts find use in nearly all aspects of ethylene polymerization, from the production of high-density polyethylene (HDPE)[1,2] and high-purity α-olefin oligomers[3] to the selective formation of 1-hexene.[4] Over the past several years, discrete organochromium complexes containing cyclopentadienyl (Cp)[5] and *anionic* non-Cp ligands[6] have produced effective polymerization catalysts, with the ligand structure exhibiting tremendous control over catalyst activity and polymer properties. Recently, *neutral* ligands have begun to figure prominently in chromium(III)-based catalysts (Chart 1). For example, Wasserscheid and McGuinness described meridianally coordinated (*mer*) octahedral chromium(III) aminebis(thioether) (**1**) and aminebis(phosphine) (**2**) complexes that, in combination with methylalumoxane (MAO), selectively trimerized ethylene to 1-hexene.[7] While the X-ray structures of **2** with R = phenyl and R = cyclohexyl were quite similar, the phenyl derivative's polymerization activity was 15 times greater than that with R = cyclohexyl, leading the authors to speculate that the active catalyst was coordinated in a manner (i.e., facially) that was sensitive to steric bulk.[7]

Chart 1

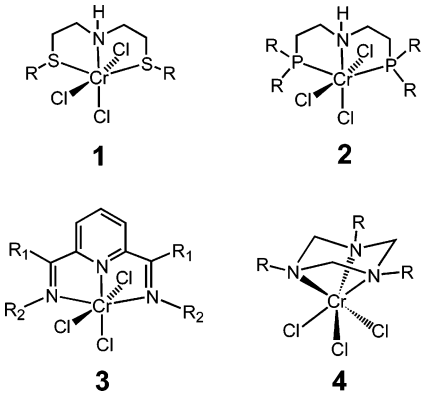

A few chromium(III) compounds with neutral triaza ligands are also known. For example, Small[8a] and

* To whom correspondence should be addressed. E-mail: carneymj@uwec.edu. Phone: 715-836-3500. Fax: 715-836-4979.
† University of Wisconsin−Eau Claire.
‡ University of California−San Diego.

(1) Chromium oxide-based catalysts for ethylene polymerization: (a) Hogan, J. P. *J. Polym. Sci., Polym. Chem. Ed*. **1970**, *8*, 2637. (b) McDaniel, M. P. *Adv. Catal*. **1985**, *33*, 47−96.

(2) Chromocene-based catalysts for ethylene polymerization: (a) Karol, F. J.; Karapinka, G. L.; Wu, C.; Dow, A. W.; Johnson, R. N.; Carrick, W. L. *J. Polym. Sci., Polym. Chem. Ed*. **1972**, *10*, 2621−2637. (b) Karol, F. J.; Brown, G. L.; Davison, J. M. *J. Polym. Sci., Polym. Chem. Ed*. **1973**, *11*, 413−424.

(3) A chromium bis(amidinate) complex is described in a patent to Chevron: Baralt, E. J.; Carney, M. J.; Cole, J. B. (Chevron Research and Technology Company) Olefin Oligomerization Catalyst and Process Employing and Preparing Same. US Patent 5,780,698, 1998.

(4) Chromium-pyrrolyl compounds are disclosed in patents to Phillips Petroleum Company: (a) Reagan, W. K.; Freemann, J. W.; Conroy, R. K.; Pettijohn, T. M.; Benham, E. A. (Phillips Petroleum Company) European Patent Application EP 0608447A1, 1993. (b) Lashier, M. E. (Phillips Petroleum Company) European Patent Application EP 0780353A1, 1997.

(5) For general overviews of Cp-chromium chemistry see: (a) Theopold, K. H. *Acc. Chem. Res.* **1990**, *23*, 263−270. (b) Theopold, K. H. *Eur. J. Inorg. Chem.* **1998**, 15−24. (c) Theopold, K. H. *CHEMTECH* **1997**, *27* (10), 26−32. (d) Pariya, C.; Theopold, K. H. *Curr. Sci.* **2000**, *78*, 1345−1351.

(6) (a) Gibson, V. C.; Spitzmesser, S. K. *Chem. Rev*. **2003**, *103*, 283−316. (b) Britovsek, G. J. P.; Gibson, V. C.; Wass, D. F. *Angew. Chem., Int. Ed*. **1999**, *38*, 428−447.

(7) McGuinness, D. S.; Wasserscheid, P.; Keim, W.; Hu, C.; Englert, U.; Dixon, J. T.; Grove, C. *Chem. Commun*. **2003**, 334−335.

10.1021/om0494162 CCC: $27.50
Publication on Web 11/25/2004

Scheme 1

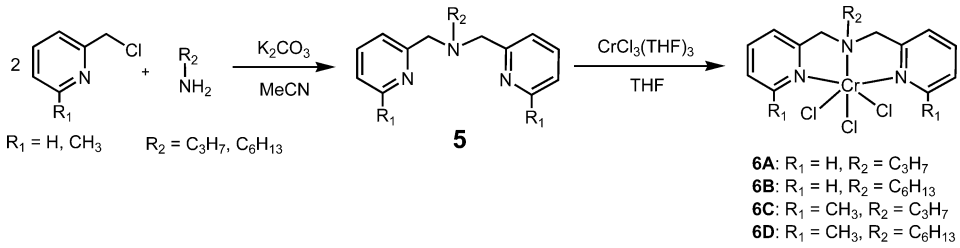

Esterueles[8b] separately reported that chromium(III) pyridinebis(imine) (PBI) complexes (**3**), after activation by MAO, polymerized ethylene to polyethylene and/or shorter chain olefins depending on the location and steric bulk of N-aryl substituents. While the *mer* geometry of **3** is enforced by the planar PBI ligand, the known reactivity of PBI with metal alkyls[9] casts some doubt on the exact catalyst structure after MAO activation. For example, Gambarotta showed that related vanadium(III) PBI complexes undergo pyridine ring alkylation under typical catalyst activation conditions and that the alkylated (now anionic) ligand binds with pseudo-facial (*fac*) geometry.[10] Other known triaza compounds include the *fac*-1,3,5-triazacyclohexane chromium(III) complexes (**4**), which were shown by Köhn to be effective olefin polymerization and oligomerization catalysts.[11] Whereas the geometry of **3** might be altered during catalyst activation (due to ligand reactivity), it is likely that the facial geometry of **4** (with its saturated 1,3,5-triazacyclohexane framework) is maintained under polymerization conditions.

We are interested in using nitrogen-based ligands to prepare early transition metal complexes and in studying the impact of ligand geometry on olefin polymerization catalysis. Recently, we reported the synthesis, X-ray structural characterization, and polymerization behavior of chromium compounds supported by the neutral tetraaza ligand tris(2-pyridylmethyl)amine (TPA).[12] The TPA-ligated chromium complexes were found to be moderately active polymerization catalysts in the presence of MAO, yielding low to moderate molecular weight HDPE. Subsequently, we have focused our efforts on compounds containing sterically less demanding bis(2-pyridylmethyl)alkylamine (**5**, BPA) ligands. Herein we report that a modest change in the BPA framework, specifically at the 6-position of the pyridine ring, alters the resulting chromium complexes' stereochemistry from *fac* to *mer*. Furthermore, we present polymerization data showing that the *fac* derivatives are significantly more active polymerization catalysts than the corresponding *mer*-ligated complexes.

Results and Discussion

The BPA ligand family (**5**) is prepared as outlined in Scheme 1,[13] and the products are isolated as yellow to orange oils after vacuum distillation. Six-coordinate chromium(III) trichloride complexes (**6**) are prepared in high yield by treatment of the appropriate BPA ligand with 1 equiv of $CrCl_3(THF)_3$ (Scheme 1). These complexes are soluble in acetonitrile and dichloromethane but only sparingly soluble in tetrahydrofuran. Electronic absorption spectra show two broad but clearly discernible ligand field transitions for each complex ($\epsilon = 70-130\ M^{-1}\ cm^{-1}$), which appear at 460 and 635 nm in **6A** and **6B** and at 472 and 672 nm in **6C** and **6D**, yielding emerald green (*fac*) and blue-green (*mer*) complexes. In the solid state, the complexes exhibit magnetic moments characteristic of the expected $S = 3/2$ ground spin state ($\mu_{eff} = 3.4$ to 3.9 μ_B) for chromium(III) centers.

X-ray crystallographic data for complexes **6A**−**6D** are presented in Table 1; important distances and angles are collected in Table 2. The crystallographic studies reveal that substitution at the 6-position of the pyridine ring influences the overall complex geometry, with unsubstituted and 6-methyl-substituted ligands forming *fac* (**6A** and **6B**) and *mer* (**6C** and **6D**) geometries, respectively. As shown in Figure 1, complexes **6A** and **6B** are best described as pseudo-octahedral chromium(III) ions, facially capped by the tridentate ligand. The resulting Cr−N bond lengths span a relatively narrow range, with the Cr−N(amine) bonds (2.131(6) Å for **6A** and 2.150(3) Å for **6B**) being ca. 0.05 Å longer than the Cr−N(pyridyl) linkages. For both complexes, the Cr−Cl bond lengths are typical for chromium(III) compounds, and there is no clear distinction between the length of Cr−Cl bonds opposite pyridyl and amine groups.

In contrast to **6A** and **6B**, complexes **6C** and **6D** display meridianal geometry with the three BPA nitrogen atoms and one chloride ligand situated in the equatorial plane (Figure 2). For each complex, the three Cr−N distances are similar, with the Cr−N(amine) bonds now slightly shorter (0.02 Å) than the Cr−N(pyridyl) bond lengths. Although the *mer* coordination geometry necessarily partitions the chlorides into axial and equatorial ligands, there is no clear distinction between the $Cr-Cl_{ax}$ and $Cr-Cl_{eq}$ bond lengths. The most significant structural feature of both **6C** and **6D** involves a twisting of the pyridine rings out of the equatorial plane. For **6C**, this twisting causes methyl carbons atoms C(13) and C(14) to be displaced 1.18 and 1.33 Å, respectively, out of the equatorial plane. For **6D**,

(8) (a) Small, B. L.; Carney, M. J.; Holman, D. M.; O'Rourke, C. E.; Halfen, J. A. *Macromolecules* **2004**, *37*, 4375−4386. (b) Esteruelas, M. A.; López, A. M.; Méndez, L.; Oliván, M.; Oñate, E. *Organometallics* **2003**, *22*, 395−406.

(9) Clentsmith, G. K. B.; Gibson, V. C.; Hitchcock, P. B.; Kimberley, B. S.; Rees, C. W. *Chem. Commun*. **2002**, 1498−1499.

(10) Reardon, D.; Conan, F.; Gambarotta, S.; Yap, G.; Wang, Q. *J. Am. Chem. Soc*. **1999**, *121*, 9318−9325.

(11) (a) Köhn, R. D.; Haufe, M.; Mihan, S.; Lilge, D. *Chem. Commun*. **2000**, 1927−1928. (b) Köhn, R. D.; Haufe, M.; Kociak-Köhn, G.; Grimm, S.; Wasserscheid, P.; Keim, W. *Angew. Chem., Int. Ed.* **2000**, *39*, 4337−4339. (c) Wasserscheid, P.; Grimm, S.; Köhn, R. D.; Haufe, M. *Adv. Synth. Catal*. **2001**, *343*, 814−818.

(12) Robertson, N. J.; Carney, M. J.; Halfen, J. A. *Inorg. Chem*. **2003**, *42*, 6876−6885.

(13) de Bruin, B.; Brands, J. A.; Donners, J. J. J. M.; Donners, M. P. J.; de Gelder, R.; Smits, J. M. M.; Gal, A. W.; Spek, A. L. *Chem. Eur. J.* **1999**, *5*, 2921−2936.

Table 1. Summary of X-ray Crystallographic Data for Chromium(III)-BPA Complexes[a]

	6A	6B	6C	6D
empirical formula	$C_{15}H_{15}Cl_3CrN_3$	$C_{18}H_{25}Cl_3CrN_3$	$C_{19}H_{26}Cl_3CrN_4$	$C_{20}H_{29}Cl_3CrN_3$
fw	399.69	441.76	468.79	469.81
cryst syst	monoclinic	monoclinic	triclinic	orthorhombic
space group	$P2_1/n$	$P2_1/n$	$P\bar{1}$	$P2_12_12_1$
a (Å)	11.874(3)	12.450(2)	8.375(8)	11.896(1)
b (Å)	11.629(3)	7.039(1)	8.914(8)	12.036(2)
c (Å)	14.032(2)	24.024(2)	15.176(14)	15.359(2)
α (deg)	90	90	104.68(2)	90
β (deg)	114.85(2)	96.01(1)	97.136(17)	90
γ ($\delta\epsilon\gamma$)	90	90	97.041(17)	90
V (Å^3)	1758.1(7)	2093.8(5)	1073.4(17)	2199.1(5)
Z	4	4	2	4
temp, K	298	298	223	298
d_{calcd} (Mg·m^{-3})	1.510	1.401	1.450	1.419
cryst size (mm)	0.35 × 0.20 × 0.04	0.45 × 0.12 × 0.10	0.30 × 0.20 × 0.10	0.38 × 0.30 × 0.28
abs coeff (mm^{-1})	1.105	0.935	0.918	0.895
$2\theta_{max}$ (deg)	49.92	49.98	46.50	49.98
transmn range	0.593−0.354	1.0−0.9205	0.914−0.770	*c*
no. of reflns collected	3239	3861	5673	15 397
no. of indep reflns	3081	3679	3073	3862
no. of obsd reflns	1615	2758	2801	3598
no. of variables	199	254	348	248
R1 (wR2)[b] [$I > 2\sigma(I)$]	0.0730 (0.1479)	0.0531 (0.0924)	0.0268 (0.0740)	0.0259 (0.0648)
goodness-of-fit (F^2)	0.982	1.050	1.046	1.028
diff peaks (e$^-$·Å^{-3})	0.536, −0.599	0.272, −0.325	0.275, −0.229	0.187, −0.375

[a] See Experimental Section for additional data collection, reduction, and structure solution and refinement details. [b] $R1 = \sum||F_o| - |F_c||/\sum|F_o|$; $wR2 = [\sum[w(F_o^2 - F_c^2)^2]]^{1/2}$ where $w = 1/\sigma^2(F_o^2) + (aP)^2 + bP$. [c] No correction for absorption was applied, as the calculated maximum and minimum transmission coefficients differed by less than 5%.

methyl carbon atoms C(7) and C(14) are displaced by 1.14 and 1.11 Å, respectively. These distortions presumably result from steric interactions between the 6-methyl groups and the orthogonal array of chloride donors.

Data from low-pressure ethylene polymerization studies (Table 3) demonstrate that ligand structure and the coordination geometry described above have a large impact on catalyst activity. Due to the low solubility of **6A**−**6D** in toluene, polymerizations were performed in dichloromethane and dichloroethane. The choice of polymerization solvent does not dramatically impact catalyst activity (compare runs 2 and 5 vs 3 and 6); however, polymers formed in dichloromethane (runs 3 and 6) have more uniform molecular weight than those produced in dichloroethane, as evidenced by the lower M_w/M_n values. Nevertheless, the most significant result is that *fac* complexes **6A** and **6B** (runs 2 and 5) display approximately 30−40 times higher activity than *mer* derivatives **6C** and **6D** (runs 7 and 8) under the same polymerization conditions. Furthermore, gel permeation chromatography (GPC) demonstrates that *fac* complexes **6A** and **6B** produce a prominent low molecular weight component (centered at about MW = 800) in dichloroethane, along with moderate amounts of higher molecular weight material (Figure 3). In contrast, polymers from *mer* derivatives **6C** and **6D** produce less of the low molecular weight fraction, a trend that is especially noticeable when comparing polymers produced by **6B** and **6D**. This low molecular weight component was not observed for polymers formed in dichloromethane. Finally, catalysts were 20−50% more active at 25 °C than at 40 °C (compare runs 1 and 4 with 2 and 5), perhaps indicative of catalyst decomposition at elevated temperatures.

Although the observed activities are somewhat modest,[14] the clear distinction between *fac* and *mer* complexes is striking, suggesting that coordination geometry (*fac* versus *mer*) exerts control over catalyst activity. To

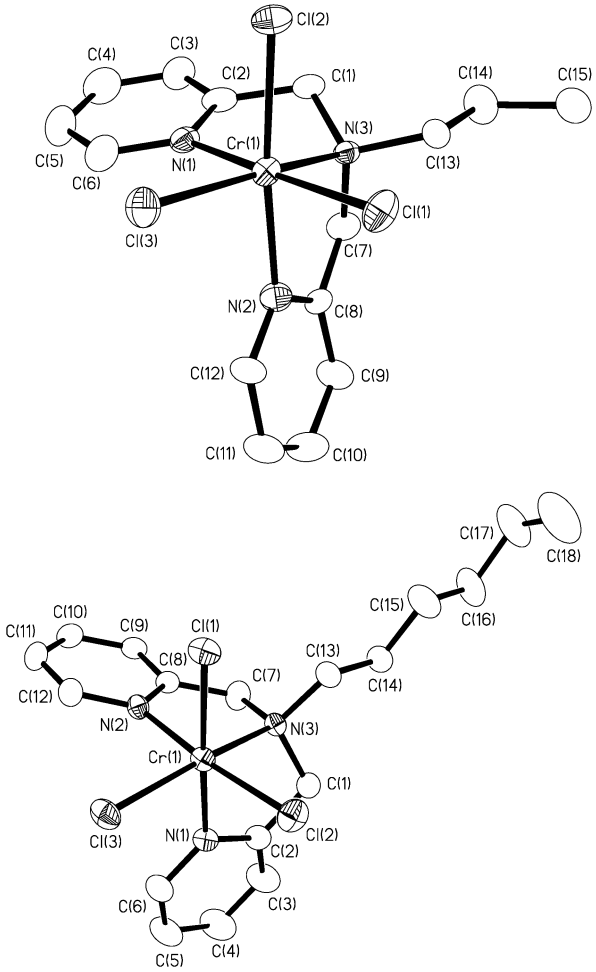

Figure 1. Thermal ellipsoid representations (35% probability boundaries) of the X-ray crystal structures of **6A** (top) and **6B** (bottom), with hydrogen atoms omitted for clarity.

Table 2. Selected Distances (Å) and Angles (deg) for Structurally Characterized Complexes

		6A	
Cr(1)−N(1)	2.090(6)	N(1)−Cr(1)−Cl(3)	92.2(2)
Cr(1)−N(2)	2.077(7)	N(2)−Cr(1)−Cl(1)	86.2(2)
Cr(1)−N(3)	2.131(6)	N(2)−Cr(1)−Cl(2)	172.8(2)
Cr(1)−C1(1)	2.301(2)	N(2)−Cr(1)−Cl(3)	92.7(2)
Cr(1)−Cl(2)	2.312(2)	N(3)−Cr(1)−Cl(1)	97.14(17)
Cr(1)−Cl(3)	2.330(2)	N(3)−Cr(1)−Cl(2)	92.18(17)
N(1)−Cr(1)−N(2)	92.2(3)	N(3)−Cr(1)−Cl(3)	167.28(17)
N(1)−Cr(1)−N(3)	77.1(2)	Cl(1)−Cr(1)−Cl(2)	92.23(9)
N(2)−Cr(1)−N(3)	81.0(2)	Cl(1)−Cr(1)−Cl(3)	93.43(9)
N(1)−Cr(1)−Cl(1)	174.2(2)	Cl(2)−Cr(1)−Cl(3)	94.45(9)
N(1)−Cr(1)−Cl(2)	88.63(18)		
		6B	
Cr(1)−N(1)	2.100(3)	N(1)−Cr(1)−Cl(3)	91.06(9)
Cr(1)−N(2)	2.073(3)	N(2)−Cr(1)−Cl(1)	85.76(9)
Cr(1)−N(3)	2.150(3)	N(2)−Cr(1)−Cl(2)	173.37(9)
Cr(1)−C1(1)	2.3239(12)	N(2)−Cr(1)−Cl(3)	92.74(9)
Cr(1)−Cl(2)	2.3065(12)	N(3)−Cr(1)−Cl(1)	95.09(9)
Cr(1)−Cl(3)	2.3155(12)	N(3)−Cr(1)−Cl(2)	92.40(9)
N(1)−Cr(1)−N(2)	89.69(12)	N(3)−Cr(1)−Cl(3)	167.34(9)
N(1)−Cr(1)−N(3)	77.89(12)	Cl(1)−Cr(1)−Cl(2)	93.22(5)
N(2)−Cr(1)−N(3)	81.17(12)	Cl(1)−Cr(1)−Cl(3)	95.51(4)
N(1)−Cr(1)−Cl(1)	172.17(9)	Cl(2)−Cr(1)−Cl(3)	93.88(5)
N(1)−Cr(1)−Cl(2)	90.57(9)		
		6C	
Cr(1)−N(1)	2.136(3)	N(1)−Cr(1)−Cl(3)	91.96(6)
Cr(1)−N(2)	2.120(3)	N(2)−Cr(1)−Cl(1)	171.38(5)
Cr(1)−N(3)	2.142(2)	N(2)−Cr(1)−Cl(2)	95.97(5)
Cr(1)−C1(1)	2.325(2)	N(2)−Cr(1)−Cl(3)	87.28(5)
Cr(1)−Cl(2)	2.309(2)	N(3)−Cr(1)−Cl(1)	101.68(6)
Cr(1)−Cl(3)	2.357(2)	N(3)−Cr(1)−Cl(2)	89.83(6)
N(1)−Cr(1)−N(2)	78.98(7)	N(3)−Cr(1)−Cl(3)	90.73(6)
N(1)−Cr(1)−N(3)	157.81(7)	Cl(1)−Cr(1)−Cl(2)	92.62(3)
N(2)−Cr(1)−N(3)	79.15(7)	Cl(1)−Cr(1)−Cl(3)	84.13(3)
N(1)−Cr(1)−Cl(1)	100.50(5)	Cl(2)−Cr(1)−Cl(3)	176.75(2)
N(1)−Cr(1)−Cl(2)	88.73(6)		
		6D	
Cr(1)−N(1)	2.140(2)	N(1)−Cr(1)−Cl(3)	87.66(6)
Cr(1)−N(2)	2.159(2)	N(2)−Cr(1)−Cl(1)	89.49(6)
Cr(1)−N(3)	2.158(2)	N(2)−Cr(1)−Cl(2)	100.59(6)
Cr(1)−C1(1)	2.3205(7)	N(2)−Cr(1)−Cl(3)	91.39(6)
Cr(1)−Cl(2)	2.3189(8)	N(3)−Cr(1)−Cl(1)	91.30(6)
Cr(1)−Cl(3)	2.3225(8)	N(3)−Cr(1)−Cl(2)	101.47(6)
N(1)−Cr(1)−N(2)	78.84(8)	N(3)−Cr(1)−Cl(3)	89.30(6)
N(1)−Cr(1)−N(3)	79.13(8)	Cl(1)−Cr(1)−Cl(2)	90.92(3)
N(2)−Cr(1)−N(3)	157.91(8)	Cl(1)−Cr(1)−Cl(3)	176.12(3)
N(1)−Cr(1)−Cl(1)	96.21(6)	Cl(2)−Cr(1)−Cl(3)	85.21(3)
N(1)−Cr(1)−Cl(2)	172.84(6)		

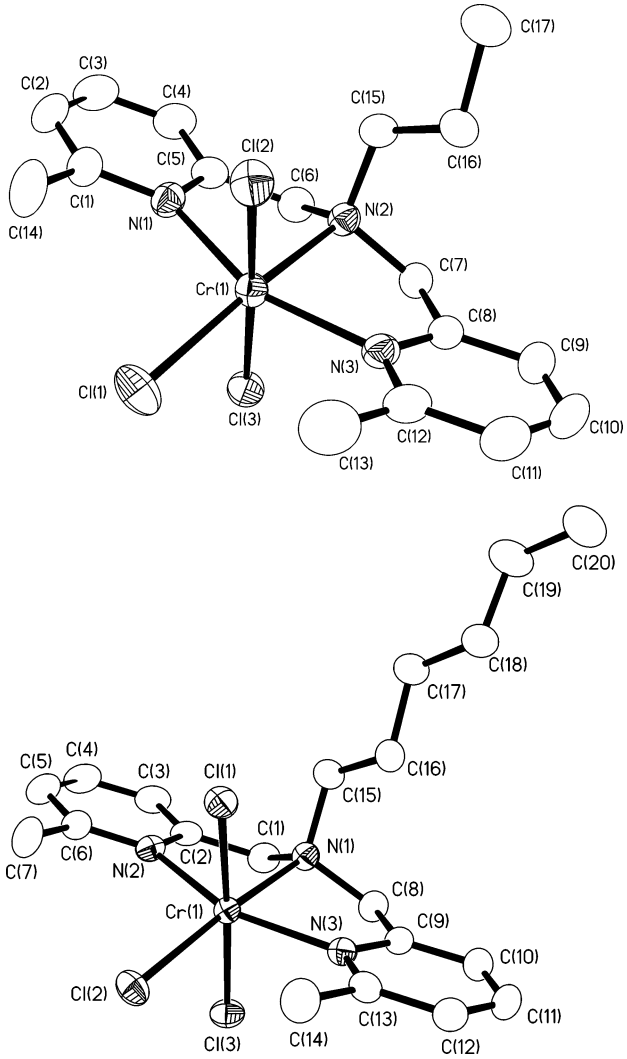

Figure 2. Thermal ellipsoid representations (35% probability boundaries) of the X-ray crystal structures of **6C** (top) and **6D** (bottom), with hydrogen atoms omitted for clarity.

our knowledge, *fac*−*mer* coordination geometry/catalyst performance studies are somewhat rare. In one example, Brookhart reported that *mer*-rhodium(III) PBI complexes did not polymerize ethylene,[15] whereas Flood found that *fac*-rhodium(III) triazacyclononane compounds were active ethylene polymerization catalysts, although no quantitative activity measures were given.[16] Brookhart suggested that the activity difference might be due to *fac* versus *mer* ligation;[15] however, the significant electronic differences between the π-accepting PBI and σ-donating triazacyclononane should also be considered. In addition, Schrock noted performance differences between five-coordinate zirconium catalysts supported by tridentate diamido/donor ligands (where donor = O, S, NR, PR),[17] with *fac* isomers typically yielding higher activity than their *mer* counterparts. With regard to the activity differences in our present study, it is possible that facially ligated **6A** and **6B** exhibit enhanced activity due to the presence of a third mutually *cis* coordination site, which could stabilize an agostic C−H interaction (α-, β-, or γ-C−H bond of the polymer chain), thus facilitating olefin insertion. Such agostic interactions have been shown by theoretical calculations to be vital to the olefin insertion process.[18] An alternative explanation for the observed activity difference is that the sterically demanding pyridyl 6-methyl groups in **6C** and **6D** might hinder olefin binding and insertion at the chromium center, reducing the ability of these catalysts to polymerize ethylene. To

(14) Although the catalysts are moderately active under low-pressure conditions, a polymerization performed in heptane at 30 °C and 400 psi (Al:Cr = 500) yielded a catalyst activity of 1.0×10^6 g PE/mol Cr·h. Data courtesy of ChevronPhillips Chemical Company.

(15) Dias, E. L.; Brookhart, M.; White, P. S. *Organometallics* **2000**, *19*, 4995−5004.

(16) (a) Wang, L.; Flood, T. C. *J. Am. Chem. Soc.* **1992**, *114*, 3169−3170. (b) Wang, L.; Lu, R. S.; Bau, R.; Flood, T. C. *J. Am. Chem. Soc.* **1993**, *115*, 6999−7000.

(17) (a) Schrock, R. R.; Seidel, S. W.; Schrodi, Y.; Davis, W. M. *Organometallics* **1999**, *18*, 428−437. (b) Graf, D. D.; Schrock, R. R.; Davis, W. M.; Stumpf, R. *Organometallics* **1999**, *18*, 843−852. (c) Baumann, R.; Stumpf, R.; Davis, W. M.; Liang, L.-C.; Schrock, R. R. *J. Am. Chem. Soc.* **1999**, *121*, 7822−7836.

(18) (a) Margl, P.; Deng, L.; Ziegler, T. *J. Am. Chem. Soc.* **1998**, *120*, 5517−5525. (b) Schmid, R.; Ziegler, T. *Organometallics* **2000**, *19*, 2756−2765. (c) Deng, L.; Schmid, R.; Ziegler, T. *Organometallics* **2000**, *19*, 3069−3076.

Table 3. Results of Polymerization Experiments[a]

run	catalyst syst	temp (°C)	catalyst amount (μmol)	solvent	Al:Cr (mol ratio)	polymer yield (g)	activity (g PE/mol Cr·h)	M_w	M_w/M_n
1	**6A**, MAO	25	50	$C_2H_4Cl_2$	200	1.09	2.2×10^4	33 200	42.8
2	**6A**, MAO	40	50	$C_2H_4Cl_2$	200	0.74	1.5×10^4	49 200	48.9
3	**6A**, MAO	40	50	CH_2Cl_2	200	0.71	1.4×10^4	114 000	16.1
4	**6B**, MAO	25	50	$C_2H_4Cl_2$	200	1.18	2.4×10^4	74 100	61.8
5	**6B**, MAO	40	50	$C_2H_4Cl_2$	200	0.99	2.0×10^4	110 000	76.1
6	**6B**, MAO	40	50	CH_2Cl_2	200	0.87	1.7×10^4	82 000	14.5
7	**6C**, MAO	40	50	$C_2H_4Cl_2$	200	0.02	4.0×10^2	147 000	25.0
8	**6D**, MAO	40	50	$C_2H_4Cl_2$	200	0.03	6.0×10^2	142 000	71.9

[a] Typical polymerization conditions: chromium complex dissolved in 100 mL of solvent, 20 psi, 1 h.

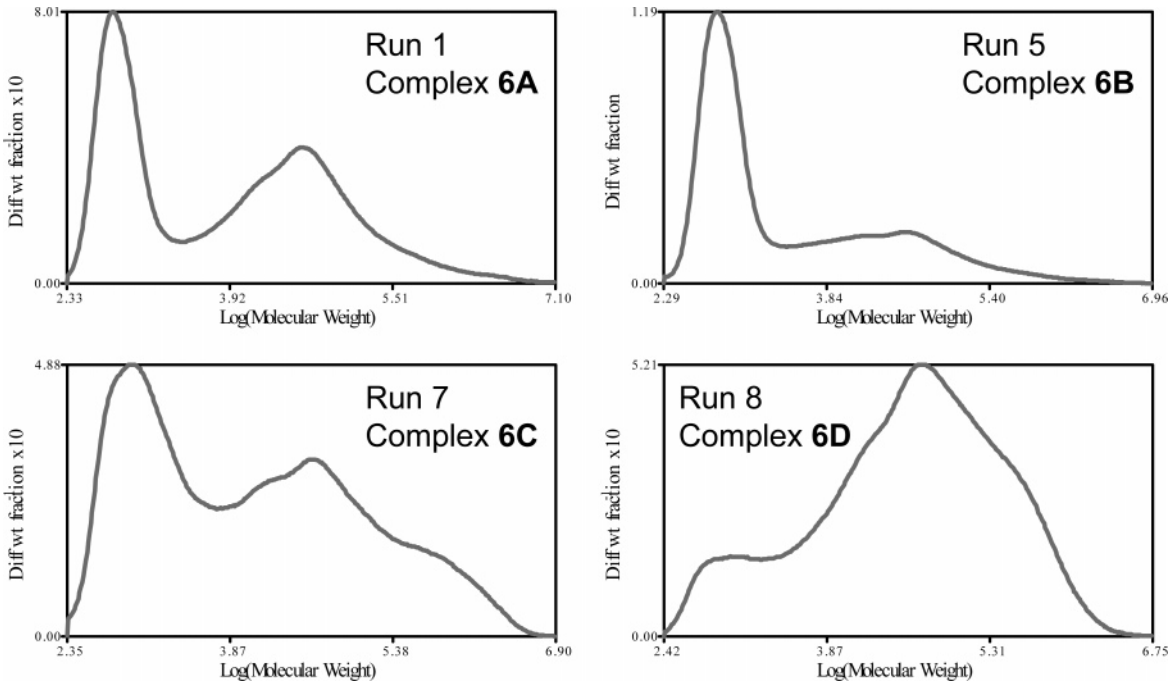

Figure 3. Gel permeation chromatography traces (refractive index plots) for polymers produced by complexes **6A**−**6D**.

help resolve this issue, we are currently preparing and testing chromium(III) compounds ligated by sterically unencumbered triaza ligands that strictly enforce *fac* and *mer* geometries.

Summary

We have prepared a family of new octahedral chromium(III) complexes supported by the BPA ligand framework. A significant discovery is that unsubstituted and 6-methyl-substituted ligands produce *fac* (**6A** and **6B**) and *mer* (**6C** and **6D**) chromium compounds, respectively, and that the *fac* derivatives are 30−40 times more active polymerization catalysts than their *mer* counterparts. This study offers a relatively rare glimpse into the impact of octahedral coordination geometry on polymerization catalyst activity. We continue to explore the role of ligand and metal complex structure on catalyst performance and are expanding our studies to include other trivalent transition metal centers and nitrogen-based ligands containing oxygen, sulfur, and phosphorus heteroatoms. In this regard, preliminary results on vanadium(III) complexes supported by BPA ligands **5A**−**5D** show a similar preference for *fac* and *mer* geometries, as well as reduced polymerization activity for the *mer* isomers.

Experimental Section

General Considerations. Unless otherwise stated, all operations were carried out under argon in a glovebox or using standard Schlenk techniques. Tetrahydrofuran, diethyl ether, dichloromethane, and acetonitrile were purified by standard drying procedures and distilled under argon prior to use. Furthermore, acetonitrile was stored over activated molecular sieves in the glovebox. Chromium(III) chloride tris(tetrahydrofuran)[19] and 2-chloromethyl-6-methylpyridine hydrochloride[20] were prepared as described in the literature. Atlantic Microlab, Inc. (Norcross, GA) performed elemental analyses. NMR spectra were obtained using a JEOL Eclipse 400 spectrometer at room temperature. Magnetic susceptibilities were determined at room temperature using a Johnson Matthey magnetic susceptibility balance, and electronic absorption spectra were recorded on a Hewlett-Packard 8453 diode array spectrophotometer (190−1100 nm range). Samples for IR were dispersed in KBr, and spectra were recorded on a Nicolet 5DXC spectrometer with a diffuse reflectance (DRIFTS) attachment. GPC measurements were performed by the analytical department at W. R. Grace with a Waters 150 C GPC operating at 140 °C using 1,2,4-trichlorobenzene as solvent.

Synthesis of *N*-Propyl-*N*,*N*-di(2-pyridylmethyl)amine (5A). Picolyl chloride hydrochloride (4.09 g, 24.9 mmol) and propylamine (0.69 mL, 8.3 mmol) were dissolved in 100 mL of

(19) Herwig, W.; Zeiss, H. H. *J. Org. Chem.* **1958**, *23*, 1404.
(20) Baker, W.; Buggle, K. M.; McOmie, J. F. W.; Watkins, D. A. M. *J. Chem. Soc.* **1958**, 3595−3603.

dry acetonitrile and treated with potassium carbonate (12 g) and tetra-*n*-butylammonium bromide (0.100 g). The resulting mixture was refluxed for 3 days, yielding a red-brown slurry. The slurry was filtered and the solvent was removed under vacuum. The resulting thick red-brown oil was treated with 30 mL of 1 M NaOH and extracted with 3 × 30 mL of dichloromethane. After removal of solvent, the product was distilled at 180 °C (0.10 Torr), yielding 1.51 g (76% based on propylamine) of orange oil. ^{1}H NMR (400 MHz, $CDCl_3$): δ 8.49 (d, J = 4.7 Hz, 2H; Py-H6), 7.62 (t, J = 7.7 Hz, 2H; Py-H4), 7.52 (d, J = 8.1 Hz, 2H; Py-H3), 7.10 (t, J = 6.2 Hz, 2H; Py-H5), 3.78 (s, 4H: N-*CH*$_2$-Py), 2.48 (t, J = 7.3 Hz, 2H; *CH*$_2$-C_2H_5), 1.52 (m, J = 7.3 Hz, 2H; CH_2-*CH*$_2$-CH_3), 0.83 (t, J = 7.4 Hz, 3H; C_2H_4-*CH*$_3$). ^{13}C{^{1}H} NMR (100 MHz, $CDCl_3$): δ 160.23, 148.93, 136.32, 122.79, 121.81, 60.54, 56.50, 20.31, 11.86.

Synthesis of *N*-Hexyl-*N*,*N*-di(2-pyridylmethyl)amine (5B). Using the general procedure outlined for **5A**, except using 3.94 g (24.0 mmol) of picolyl chloride hydrochloride and 1.05 mL (8.0 mmol) of hexylamine, 2.22 g (99% based on hexylamine) of product was isolated as an orange oil after distillation at 195 °C (0.10 Torr). ^{1}H NMR (400 MHz, $CDCl_3$): δ 8.46 (d, J = 4.8 Hz, 2H; Py-H6), 7.59 (t, J = 7.5 Hz, 2H; Py-H4), 7.49 (d, J = 8.1 Hz, 2H; Py-H3), 7.07 (t, J = 6.2 Hz, 2H; Py-H5), 3.76 (s, 4H: N-*CH*$_2$-Py), 2.48 (t, J = 7.5 Hz, 2H; *CH*$_2$-C_5H_{11}), 1.48 (m, J = 7.3 Hz, 2H; CH_2-*CH*$_2$-C_4H_9), 1.24−1.14 (m, 6H; C_2H_4-*CH*$_2$-C_3H_7, C_3H_6-*CH*$_2$-C_2H_5, C_4H_8-*CH*$_2$-CH_3), 0.79 (t, J = 7.0 Hz, 3H; C_5H_{10}-*CH*$_3$). ^{13}C{^{1}H} NMR (100 MHz, $CDCl_3$): δ 160.27, 148.96, 136.32, 122.82, 121.82, 60.59, 54.57, 31.71, 27.12, 27.03, 22.65, 14.08.

Synthesis of *N*-Propyl-*N*,*N*-di(6-methyl-2-pyridylmethyl)amine (5C). This compound was prepared by reaction of 3.74 g (21.0 mmol) of 2-chloromethyl-6-methylpyridine hydrochloride and 0.58 mL (7.0 mmol) of propylamine, along with potassium carbonate (12 g) and tetra-*n*-butylammonium bromide (0.100 g), in 100 mL of dry acetonitrile. The resulting mixture was refluxed for 3 days, yielding a yellow slurry, which was filtered and dried under vacuum. The resulting yellow oil was treated with 30 mL of 1 M NaOH and extracted with 3 × 30 mL of dichloromethane. After removal of solvent, product was distilled at 185 °C (0.10 Torr), to yield 1.71 g (91% based on propylamine) of pale yellow oil. ^{1}H NMR (400 MHz, $CDCl_3$): δ 7.51 (t, J = 7.7 Hz, 2H; Py-H4), 7.37 (d, J = 7.7 Hz, 2H; Py-H3), 6.96 (d, J = 7.7 Hz, 2H; Py-H5), 3.76 (s, 4H: N-*CH*$_2$-Py), 2.49−2.45 (m, 8H; *CH*$_2$-C_2H_5, Py-*CH*$_3$), 1.52 (m, J = 7.4 Hz, 2H; CH_2-*CH*$_2$-CH_3), 0.84 (t, J = 7.4 Hz, 3H; C_2H_4-*CH*$_3$). ^{13}C{^{1}H} NMR (100 MHz, $CDCl_3$): δ 159.86, 157.38, 136.54, 121.19, 119.35, 60.69, 56.49, 24.47, 20.37, 11.86.

Synthesis of *N*-Hexyl-*N*,*N*-di(6-methyl-2-pyridylmethyl)-amine (5D). Using the general procedure outlined for **5C**, except using 2.48 g (13.9 mmol) of 2-chloromethyl-6-methylpyridine hydrochloride and 0.61 mL (4.6 mmol) of hexylamine, 1.21 g (84% based on hexylamine) of product was isolated as a pale yellow oil after distillation at 195 °C (0.10 Torr). ^{1}H NMR (400 MHz, $CDCl_3$): δ 7.47 (t, J = 7.5 Hz, 2H; Py-H4), 7.32 (d, J = 7.7 Hz, 2H; Py-H3), 6.91 (d, J = 7.3 Hz, 2H; Py-H5), 3.72 (s, 4H: N-*CH*$_2$-Py), 2.47−2.44 (m, 8H; *CH*$_2$-C_5H_{11}, Py-*CH*$_3$), 1.46 (m, J = 7.3 Hz, 2H; CH_2-*CH*$_2$-C_4H_9), 1.24−1.08 (m, 6H; C_2H_4-*CH*$_2$-C_3H_7, C_3H_6-*CH*$_2$-C_2H_5, C_4H_8-*CH*$_2$-CH_3), 0.78 (t, J = 7.0 Hz, 3H; C_5H_{10}-*CH*$_3$). ^{13}C{^{1}H} NMR (100 MHz, $CDCl_3$): δ 159.73, 157.42, 136.61, 121.28, 119.52, 60.65, 54.52, 31.71, 27.05, 27.02, 24.39, 22.65, 14.08.

Synthesis of {*N*-Propyl-*N*,*N*-di(2-pyridylmethyl)amine}-$CrCl_3$ (6A). A mixture of $CrCl_3(THF)_3$ (0.635 g, 1.69 mmol) and **5A** (0.409 g, 1.69 mmol) was stirred overnight in 10 mL of tetrahydrofuran, forming a light green precipitate and faint green supernatant. The solid was isolated by filtration and washed with ca. 2 mL of tetrahydrofuran (0.659 g, 97%). Slow cooling of a saturated acetonitrile solution yielded crystals suitable for single-crystal X-ray analysis. FTIR (KBr): 3072, 3036, 2966, 2933, 2872, 1605, 1483, 1438, 1315, 1291, 1156, 1058, 1029, 911, 768, 760, 649, 425 cm^{-1}. UV−vis (CH_3CN) [λ_{max}, nm (ϵ, M^{-1} cm^{-1})]: 460 (110), 634 (75). Anal. Calc (Found) for $C_{15}H_{19}N_3Cl_3Cr$: C, 45.08 (44.94); H, 4.79 (4.76); N, 10.51 (10.46). μ_{eff} = 3.4 μ_B.

Synthesis of {*N*-Hexyl-*N*,*N*-di(2-pyridylmethyl)amine}-$CrCl_3$ (6B). In a procedure similar to that used for **6A**, ligand **5B** (0.455 g, 1.60 mmol) and $CrCl_3(THF)_3$ (0.601 g, 1.60 mmol) reacted to yield 0.624 g (88%) of green product. Slow evaporation of an acetonitrile solution yielded X-ray quality crystals. FTIR (KBr): 2950, 2925, 2852, 1605, 1569, 1487, 1450, 1413, 1291, 1160, 1058, 1025, 764, 653, 429 cm^{-1}. UV−vis (CH_3CN) [λ_{max}, nm (ϵ, M^{-1} cm^{-1})]: 460 (130), 636 (88). Anal. Calc (Found) for $C_{18}H_{25}N_3Cl_3Cr$: C, 48.94 (48.88); H, 5.70 (5.48); N, 9.51 (9.48). μ_{eff} = 3.4 μ_B.

Synthesis of {*N*-Propyl-*N*,*N*-di(6-methyl-2-pyridylmethyl)amine}$CrCl_3$·MeCN (6C). In a procedure similar to that used for **6A**, ligand **5C** (0.140 g, 0.39 mmol) and $CrCl_3(THF)_3$ (0.145 g, 0.39 mmol) combined to yield 0.152 g of a green solid. The solid was dissolved in 60 mL of acetonitrile, heated to 65 °C, filtered, and allowed to slowly cool to room temperature, forming green crystals. Further concentration yielded 0.119 g (66%) of dark green, blocklike crystals. A crystal taken from this batch was suitable for single-crystal X-ray analysis. FTIR (KBr): 2962, 2925, 2868, 1614, 1569, 1462, 1442, 1352, 1230, 1164, 1041, 1021, 919, 845, 780, 580 cm^{-1}. UV−vis (CH_3CN) [λ_{max}, nm (ϵ, M^{-1} cm^{-1})]: 472 (100), 672 (110). Anal. Calc (Found) for $C_{19}H_{27}N_4Cl_3Cr$: C, 48.17 (48.68); H, 5.73 (5.59); N, 11.76 (11.95). μ_{eff} = 3.9 μ_B.

Synthesis of {*N*-Hexyl-*N*,*N*-di(6-methyl-2-pyridylmethyl)amine}$CrCl_3$ (6D). Analogous to the procedure for **6A**, ligand **5D** (0.356 g, 1.14 mmol) and $CrCl_3(THF)_3$ (0.428 g, 1.14 mmol) reacted to form 0.439 g (82%) of green solid. Crystals suitable for X-ray diffraction studies were obtained by slowly cooling a saturated acetonitrile solution. FTIR (KBr): 3068, 2925, 2851, 1610, 1573, 1462, 1446, 1364, 1266, 1172, 1013, 849, 800, 780, 719, 584, 412 cm^{-1}. UV−vis (CH_3CN) [λ_{max}, nm (ϵ, M^{-1} cm^{-1})]: 472 (98), 672 (110). Anal. Calc (Found) for $C_{20}H_{29}N_3Cl_3Cr$: C, 51.13 (50.88); H, 6.22 (6.27); N, 8.94 (8.77). μ_{eff} = 3.6 μ_B.

X-ray Crystallography. Single-crystal specimens selected for crystallographic characterization were mounted on thin glass fibers and transferred to an Enraf-Nonius CAD4 (**6B**), a Siemens P4/CCD diffractometer (**6C**), or a Bruker-Nonius MACH3S (**6A**, **6D**) diffractometer equipped with graphite-monochromated Mo Kα radiation (λ = 0.71073 Å). Data were collected at ambient temperature for **6A**, **6B**, and **6D** and at 223 K for **6C**. For **6A**, **6B**, and **6D**, unit cell constants were determined from a least squares refinement of the setting angles of 25 machine-centered reflections located using an automated search routine. Intensity data were collected using the $\omega/2\theta$ scan technique to a maximum 2θ value of 50°. When necessary, absorption corrections were applied using azimuthal scans of several intense reflections, resulting in transmission factors ranging from 0.593 to 0.394 (**6A**), 1.0 to 0.921 (**6B**) and, by SADABS, 0.914 to 0.770 (**6C**). The data for **6A**, **6B**, and **6D** were corrected for Lorentz and polarization effects and converted to structure factors using the teXsan for Windows crystallographic software package.[21] Space groups were determined on the basis of systematic absences and intensity statistics. Structures were solved by direct methods or by the Patterson method, which provided the positions of most of the non-hydrogen atoms. The remaining non-hydrogen atoms were located after several cycles of structure expansion and full matrix least squares refinement (on F^2). All non-hydrogen atoms were refined using anisotropic displacement parameters. Hydrogen atoms in **6A**, **6B**, and **6D** were added geometrically and refined as riding atoms with group isotropic displacement parameters. In **6C**, the hydrogen atoms were

(21) *TeXan for Windows*, V 1.02; Molecular Structure Corporation, Inc.: The Woodlands, TX; 1997.

found from the F-map and refined without restrictions using isotropic thermal parameters. Refinement of **6A**, **6C**, and **6D** proceeded normally. For **6B**, a three-carbon unit (C16, C17, C18) of the hexyl group was disordered over two positions with refined site occupancy factors of 0.699 and 0.301. This disorder was treated using a split-atom model, with bond length and anisotropic displacement parameter constraints applied to the disordered atoms.

For all compounds, structure solution and refinement were performed using the SHELXTL suite of programs.[22] Relevant crystallographic information for the compounds is summarized in Table 1, and selected interatomic distances and angles are provided in Table 2. Complete crystallographic data for each compound are provided as Supporting Information in CIF format.

General Ethylene Polymerization Procedure. In a glovebox, the chromium complex precatalyst (50 μmol) was dissolved in 100 mL of solvent and placed in a Fisher-Porter bottle adapted with stainless steel valving and connections. The required amount of MAO (10 wt %) was added to this solution, and the bottle was sealed, placed in a constant temperature water bath, and connected to a constant 20 psig ethylene supply. The solution was stirred with a magnetic stir bar. Polymerizations were halted after 1 h by venting the reactor and treating the reactor contents with 30 mL of 6 M HCl and 200 mL of methanol. Solid polymeric products were collected by filtration, washed with methanol, and dried under vacuum.

(22) *SHELXTL* V. 6.12 for Windows; Bruker AXS: Madison, WI; 2001.

Acknowledgment. We thank the donors of the Petroleum Research Fund, administered by the American Chemical Society (Grant 37885-GB3 to M.J.C.), Research Corporation (Cottrell College Science Award to M.J.C.), the National Science Foundation (CHE-0078746 to J.A.H.), and the University of Wisconsin−Eau Claire for financial support of this research. Instrumentation for infrared analyses was obtained with the support of the National Science Foundation MRI (CHE-0216058). We also wish to thank the Albemarle Corporation for providing MAO, W. R. Grace (Davison Catalyst Division) for polymer analyses, and Dr. Brooke Small (ChevronPhillips Chemical Company) for high-pressure polymerization evaluations.

Supporting Information Available: Complete X-ray crystallographic information in CIF format. This material is available free of charge on the Internet at http://pubs.acs.org.

OM0494162